

## Electrochemical and XPS Study on Effect of Cl<sup>-</sup> on Corrosion Behavior of Reinforcing Steel in Simulated Concrete Pore Solutions

Ya Guo, Xiao-Ping Wang, Yan-Feng Zhu, Juan Zhang, Ying-Bo Gao, Zai-You Yang, Rong-Gui Du\* and Chang-Jian Lin

State Key Laboratory of Physical Chemistry of Solid Surfaces, Department of Chemistry, College of Chemistry and Chemical Engineering, Xiamen University, Xiamen, Fujian 361005, P. R. China

\*E-mail: [rgdu@xmu.edu.cn](mailto:rgdu@xmu.edu.cn)

Received: 5 August 2013 / Accepted: 18 September 2013 / Published: 20 October 2013

---

The effect of Cl<sup>-</sup> on the corrosion behavior of reinforcing steel in simulated concrete pore solutions was studied by the polarization curve measurements, electrochemical impedance spectroscopy, scanning electron microscopy and X-ray photoelectron spectroscopy. The results showed that the corrosion resistance of reinforcing steel was correlated with the Cl<sup>-</sup> concentration of the solutions. With the increase of the Cl<sup>-</sup> concentration, the corrosion potential of the reinforcing steel shifted negatively and its corrosion current density rose, and the Fe and Fe<sup>2+</sup> content of the steel surface film increased but the Fe<sup>3+</sup> content decreased. When the Cl<sup>-</sup> concentration reached 0.50 M in the solution, the passive film was destroyed and the localized corrosion took place on the steel surface.

---

**Keywords:** Reinforcing steel; Localized corrosion; Simulated concrete pore solution; Cl<sup>-</sup>; XPS

### 1. INTRODUCTION

The premature degradation of reinforced concrete structures due to the reinforcing steel corrosion has resulted in a huge economic loss in modern society. Therefore, the study on the corrosion behavior of the reinforcing steel is of great practical significance [1-2].

Under normal conditions, reinforcing steel in concrete can be protected from corrosion by spontaneously forming a compact passive film on the steel surface because of the high alkalinity of the concrete pore solution. However, the protective film may become unstable and even broken due to the change of the environment that is suitable for the passivated steel. Generally, the carbonation of concrete and the penetration of Cl<sup>-</sup> are the main reasons that cause the breakdown of the passive film [3-8], which is an important part of corrosion studies for the corrosion control of reinforcing steel in

concrete. Consequently, the study on the mechanism of  $\text{Cl}^-$  inducing the steel depassivation and the critical concentration for the steel corrosion has attracted considerable attention of corrosion researchers. Due to the differences in experimental systems and measurement methods, etc., the measurement results of the critical chloride concentrations differed greatly and there was no unified conclusion [6,8-11]. Simulated concrete pore solutions are commonly used for studying the reinforcing steel corrosion behavior on account of the complexity of reinforced concrete systems [4,9,11], which is of beneficial help for understanding the corrosion mechanism of reinforcing steel.

Lewis measured polarization curves of the steel electrodes in the saturated  $\text{Ca}(\text{OH})_2$  solution in 1962, and found that the steel depassivation and corrosion occurred when the content of  $\text{NaCl}$  reached 0.05% [12]. In 1970, Gouda *et al.* measured the chloride thresholds for corrosion of reinforcing steel in the simulated concrete pore solutions with different pH values [13]. Their results showed that when pH increased from 12.0 to 13.5 in the simulated concrete pore solution, the chloride threshold increased from 0.06% to 0.3%. Moreno measured chloride threshold levels by adding  $\text{Cl}^-$  with various concentrations in the four simulated concrete pore solutions and found that pitting corrosion resistance was improved and the chloride threshold level increased in the high concentration of carbonate and bicarbonate [9]. Morris *et al.* found that chloride threshold has a lot to do with the resistance of the concrete, and its values are proportional to resistivity values [14]. Most previous measurements of chloride thresholds for reinforcing steel corrosion were carried out only by the traditional electrochemical tests in the single-component simulated concrete pore solution, namely saturated  $\text{Ca}(\text{OH})_2$  solution, and there were few studies on the mechanism of steel depassivation by  $\text{Cl}^-$  attack. Therefore, the objective of the present work is to study the influence of the  $\text{Cl}^-$  concentration on the corrosion behavior of reinforcing steel in a three-component simulated pore solution and determine its threshold value for steel corrosion by electrochemical techniques assisted by X-ray photoelectron spectroscopy (XPS) and scanning electron microscopy (SEM).

## 2. EXPERIMENTAL

The tested material was R235 reinforcing steel with chemical composition of (wt.%): C 0.390, Si 0.083, Mn 0.254, Cu 0.101, S 0.012, P 0.015, Ni 0.027 and balance Fe. The steel used in electrochemical measurements were cut into  $\text{Ø}1.12 \text{ cm} \times 0.4 \text{ cm}$  cylindrical specimens after removing its oxide scale. One of the plane surfaces was used as a working surface and a Cu lead wire was welded on the other surface. Every specimen was sealed with epoxy resin and mounted in a PVC holder only leaving a working surface of  $1.00 \text{ cm}^2$ . The size of cylindrical specimens used for SEM and XPS measurements were  $\text{Ø}5.0 \text{ mm} \times 2.0 \text{ mm}$ . Before testing, all the steel samples were wet abraded with emery papers of grade from 400 to 1500, rinsed with deionized water, then ultrasonically cleaned in ethanol for 10 min and finally dried in air.

A mixed solution of 0.6 M KOH, 0.2 M NaOH, and 0.001 M  $\text{Ca}(\text{OH})_2$  [15,16] was designated as the simulated concrete pore (SCP for short) solution and the test solution after the solution pH was adjusted to 12.50 with a 0.8 M  $\text{NaHCO}_3$  solution, The addition of  $\text{NaCl}$  was to change the

concentration of  $\text{Cl}^-$  in the test solution. All the solutions were prepared with analytical grade reagents and deionized water.

Electrochemical measurements were conducted by an Autolab Potentiostat Galvanostat in the air at the room temperature ( $25 \pm 2^\circ\text{C}$ ) after the steel specimens were immersed in the test solutions for 40 min to obtain stable corrosion potentials. A three-electrode cell was used for the measurements with the steel specimen as the working electrode, a saturated calomel electrode (SCE) as the reference electrode and a platinum electrode as the counter electrode. The Tafel polarization curves of the steel in the SCP solution were recorded in the range from -120 mV to 120 mV versus corrosion potentials at a scan rate of 0.5 mV/s. The potentiodynamic anodic polarization curves were measured from corrosion potentials in the positive direction until the polarization current density reached  $150 \mu\text{A}/\text{cm}^2$  at a scan rate of 0.8 mV/s. EIS measurements were made in a frequency range of 100 kHz to 0.01 Hz and with 10 mV amplitude of the sinusoidal voltage signal. All the fitting procedures and data processing were performed automatically by the software of Autolab.

The surface compositions of the steel specimens were characterized by XPS spectrometer (PHI Quantum 2000). The X-ray source of Al  $K\alpha$  (1486.6 eV) was set at 15 kV and 25 W. The take-off angle of the photoelectron and the incident beam diameter used in all experiments were  $45^\circ$  and 200  $\mu\text{m}$ , respectively. Binding energies were referenced to the C 1s signal at 284.8 eV. The analysis of the different depth of the steel surface was performed by  $\text{Ar}^+$  sputtering with 4 keV at a rate of 75 nm/min (based on the  $\text{SiO}_2$  standard to make calculations). In order to get more precise information, a narrow spectrum of Fe was measured by a high resolution scan. The steel surface films at 5 nm depth were analyzed by the deconvolution method to eliminate the effect of  $\text{O}_2$  and  $\text{CO}_2$  from the air and study the attack effect of  $\text{Cl}^-$  on the films.

After immersion in different test solutions for 40 min at room temperature, the surface morphology changes were observed by a field-emission scanning electron microscope (SEM, Hitachi FE-SEM S4800).

### 3. RESULTS AND DISCUSSION

#### 3.1. Tafel polarization curves

Figure 1 shows the Tafel polarization curves of the reinforcing steel immersed in the SCP solutions with different  $\text{Cl}^-$  concentrations. The fitting electrochemical parameters of the steel electrode obtained from the curves are listed in Table 1, where  $E_{\text{corr}}$  is defined as the corrosion potential,  $i_{\text{corr}}$  is the corrosion current density, and  $R_p$  represents the polarization resistance. It can be seen from Figure 1 and Table 1 that the increase in the  $\text{Cl}^-$  concentration resulted in a shift of the corrosion potential in the negative direction, an increase of the corrosion current density and a decrease in the polarization resistance. This results showed that the stability of the passive film on the steel surface was reduced and the corrosion resistance of the reinforcing steel decreases with increasing the  $\text{Cl}^-$  concentration. The  $i_{\text{corr}}$  showed the lowest value when the steel was immersed in the solution without  $\text{Cl}^-$ , indicating that the steel had the best corrosion resistance under this condition. When the steel was immersed in

the SCP solution with 0.30 M Cl<sup>-</sup>, the  $E_{\text{corr}}$  change was not remarkable, the  $R_p$  slightly decreased, and the  $i_{\text{corr}}$  showed little change and still lower than 0.1  $\mu\text{A}/\text{cm}^2$ , suggesting that the steel was still in the passive state [17-18]. After addition of 0.40 M Cl<sup>-</sup> to the solution, the  $i_{\text{corr}}$  was higher than 0.1  $\mu\text{A}/\text{cm}^2$  and was three times as high as that in the solution without Cl<sup>-</sup>, and  $R_p$  significantly decreased, which indicated that the film on the steel was not in a steady state. With the increase of the Cl<sup>-</sup> concentration to 0.50 M,  $i_{\text{corr}}$  increased considerably. After testing, the steel surface became rough, and some corrosion pits on it were observed, suggesting localized corrosion would occur on the steel surface due to its depassivation when the Cl<sup>-</sup> concentration reached a certain value.

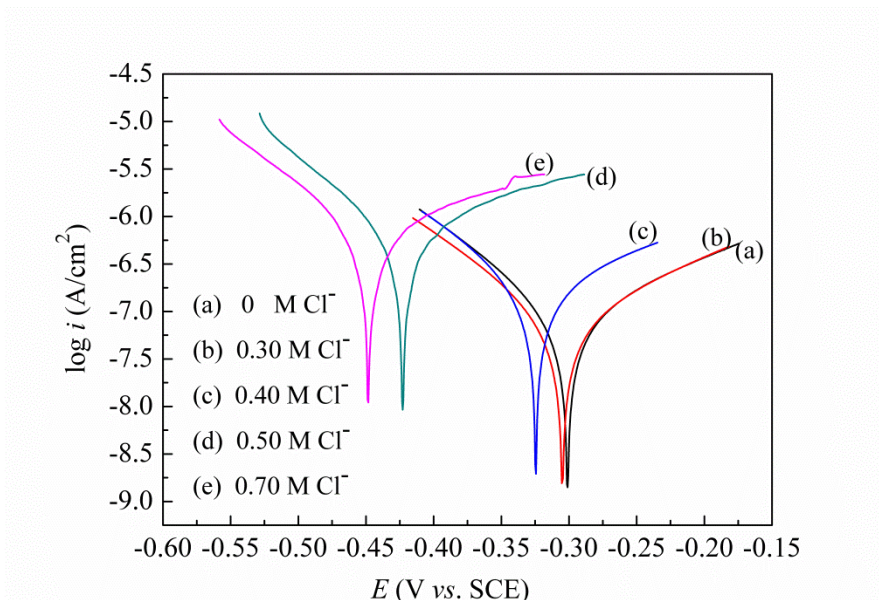


**Figure 1.** Tafel polarization curves of the reinforcing steel in the SCP solutions with different Cl<sup>-</sup> concentrations

**Table 1.** Polarization parameters for the reinforcing steel in the SCP solutions with different Cl<sup>-</sup> concentrations

Cl <sup>-</sup> concentration (M)	$i_{\text{corr}}$ ( $\mu\text{A}/\text{cm}^2$ )	$E_{\text{corr}}$ (mV vs. SCE)	$R_p$ ( $\text{k}\Omega \text{cm}^2$ )
0	0.087	-302	321.7
0.30	0.095	-306	281.1
0.40	0.267	-325	136.4
0.50	1.133	-423	34.2
0.70	1.444	-448	33.8

### 3.2. Potentiodynamic anodic polarization curves

Anodic polarization curves can provide information on passivation or depassivation of a metal immersed in solutions [9,19-21]. Figure 2 shows the potentiodynamic anodic polarization curves of the reinforcing steel immersed in the SCP solutions with different  $\text{Cl}^-$  concentrations. It can be seen that the curve (a) exhibited a stable passive region for the steel in the SCP solution without  $\text{Cl}^-$ , showing that the steel was in a passive state and was not be eroded [9,19-21]. After adding 0.30 M  $\text{Cl}^-$  to the solution, the curve (b) did not change obviously, indicating the film formed on the steel surface was not broken and the steel remained passive. When the  $\text{Cl}^-$  concentration increased to 0.40 M, the extent of the passive region in the curve (c) was reduced, indicating the corrosion resistance of the steel decreased, but it was still in a passive state at the corrosion potential [9,20,21]. The corrosion behavior of the steel varied considerably when the  $\text{Cl}^-$  concentration reached 0.50 M or higher in the SCP solution, no a stable passive region occurred in the curve (d) or (e), suggesting the  $\text{Cl}^-$  concentration exceeded a critical level for the steel corrosion because of depassivation caused by  $\text{Cl}^-$  attack [1,9,20,21]. The results from the measurement of anodic polarization curves showed the similar corrosion behavior of the reinforcing steel analyzed by the Tafel polarization. Therefore, it could be inferred that the  $\text{Cl}^-$  concentration resulting in the steel corrosion was in the range of 0.40-0.50 M.

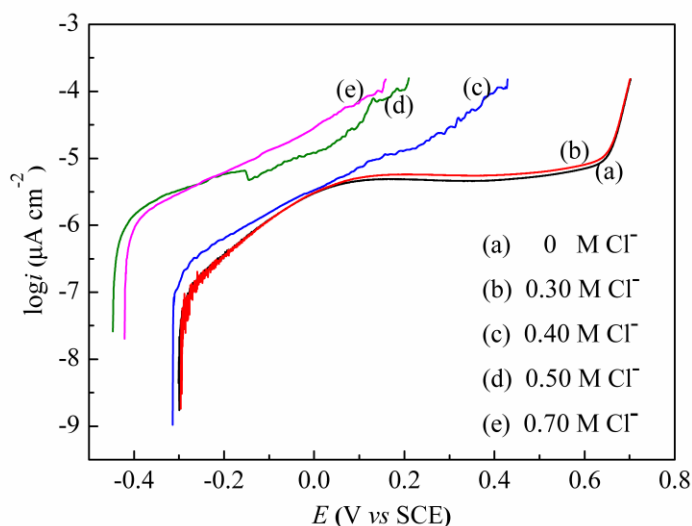


**Figure 2.** Potentiodynamic anodic polarization curves of the reinforcing steel in the SCP solutions with different  $\text{Cl}^-$  concentrations

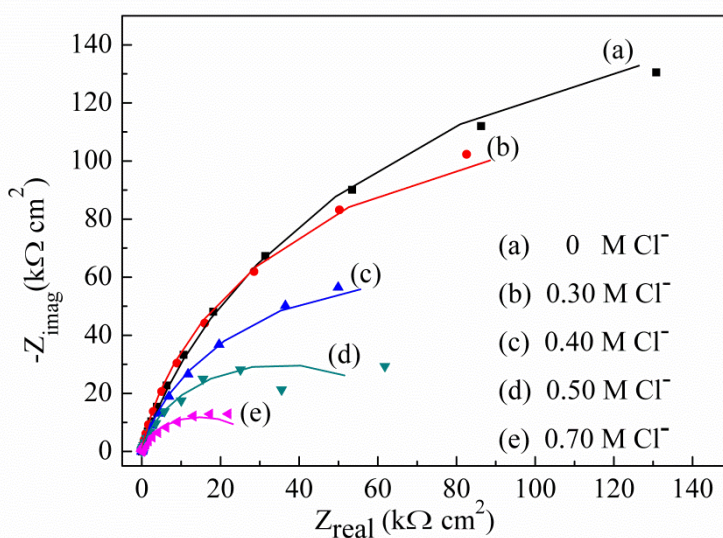
### 3.3. Electrochemical impedance spectroscopy

Figure 3 shows the Nyquist plots for the reinforcing steel in the SCP solutions with different  $\text{Cl}^-$  concentrations. The point line represents experimental data and the solid line is the fitting curve. The simulating equivalent circuit is represented in Figure 4, where  $R_s$  represents the solution resistance, and  $R_{ct}$  is the interfacial charge transfer resistance. The  $R_{ct}$  may be used for evaluating the

corrosion resistance of the reinforcing steel. Constant phase element (CPE) represents the double-layer capacitance of the steel/electrolyte interface, and  $Z_{CPE}$  can be defined as follows [22]:

$$Z_{CPE} = [Y_0(j\omega)^n]^{-1} \quad [1]$$

where  $Y_0$  is a parameter with dimensions of  $\Omega^{-1} \cdot \text{cm}^{-2} \cdot \text{s}^n$ , which is directly proportional to the double layer capacitance of pure capacitive electrodes, and it represents different quantities, which depending on the value of the exponent  $n$ . Here,  $n$  represents the deviated degree of the capacitance of the solid electrode double-layer from the ideal condition, and its value ranges from 0 to 1. For the electrode acts as a pure capacitance,  $n = 1$ , for the electrode acts as a pure resistor,  $n = 0$ . The fitting data of corresponding elements in the equivalent circuit are listed in Table 2.



**Figure 3.** Nyquist plots of the reinforcing steel in the SCP solutions with different  $\text{Cl}^-$  concentrations

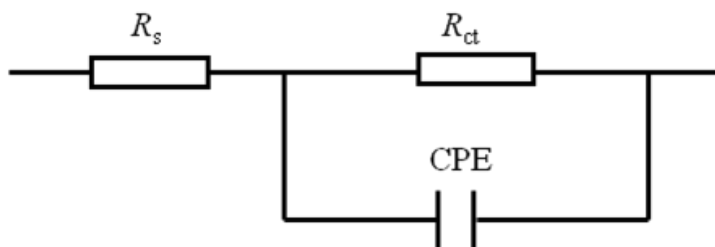


**Figure 4.** Equivalent circuit mode for the reinforcing steel in the SCP solution

As shown in Figure 3, the impedance spectra of the reinforcing steel in the SCP solution ( $\text{pH} = 12.50$ ) with a  $\text{Cl}^-$  concentration of 0.40 M or lower, the Nyquist plot consisted of only a capacitive arc and presented a time constant. We could get only an incomplete capacitive arc as the steel surface had a high charge transfer resistance and the corrosion system contained a high time constant and low

characteristic frequencies. So what we got is an incomplete capacitive reactance arc, suggesting the electrochemical corrosion was almost fully inhibited on the steel/electrolyte interface in the above condition, and the passive film was stable. When the  $\text{Cl}^-$  concentration increased to 0.50 M or higher, it can be seen from the Figure 3 (d) or (e), the impedance modulus was obviously decreased. The plot presented a capacitive reactance arc at high frequencies and it significantly shrank at the low frequencies.

**Table 2.** Impedance parameters for the reinforcing steel in the SCP solutions with different  $\text{Cl}^-$  concentrations

$\text{Cl}^-$ Concentration (M)	$R_s$ ( $\Omega \text{ cm}^2$ )	$R_{ct}$ ( $\text{k}\Omega \text{ cm}^2$ )	$Y_0$ ( $10^{-5} \Omega^{-1} \text{ cm}^{-2} \text{ s}^n$ )	$n$
0	6.22	268.8	6.47	0.93
0.30	5.24	238.0	7.14	0.92
0.40	3.81	138.6	10.45	0.88
0.50	3.49	65.8	9.37	0.89
0.70	3.21	29.9	16.30	0.85

The results showed that the passive film formed on the steel surface had been destroyed by  $\text{Cl}^-$  attack, and the steel was active. Because the  $\text{Cl}^-$  has a small radius and higher activity, it could be easily adsorbed to the steel surface defects and inclusion sites and cause the localized electrodissoolution and steel corrosion when its concentration reached a critical value [1,4,11]. The above results could be further supported by the quantified resistance values as can be seen from the fitting data of  $R_{ct}$  in Table 2.  $R_{ct}$  of the steel decreased with an increase in the  $\text{Cl}^-$  concentration in the test solutions. When the  $\text{Cl}^-$  concentration reached 0.50 M, the  $R_{ct}$  value significantly decreased, indicating the rate of electrochemical reaction on the steel surface increased greatly because of occurrence of corrosion. This result is consistent with the above polarization curve measurements.

It has been reported that the critical  $\text{Cl}^-$  concentration for the corrosion of steel was between 0.01-0.04 M when it was immersed in a saturated  $\text{Ca}(\text{OH})_2$  solution with pH of about 12.50 [23], and was between 0.028-0.17 M for that in a NaOH solution with pH of 12.60 [24]. In our test, the simulated concrete pore solution contained 0.6 M KOH, 0.2 M NaOH and 0.001 M  $\text{Ca}(\text{OH})_2$ , and the pH of the solution was adjusted to 12.50 with a 0.8 M  $\text{NaHCO}_3$  solution, the critical  $\text{Cl}^-$  concentration was 0.40~0.50 M, which is obviously higher than the former results. It suggested that the critical  $\text{Cl}^-$  concentration was related to the composition of simulated concrete pore solutions. Thomas *et al.* found that bicarbonate could affect the corrosion resistance of the passive film on the steel surface, the Flade potential of the steel decreased, and the stability of passive film was enhanced with increasing of the bicarbonate concentration [25]. The simulated concrete pore solution contained  $\text{NaHCO}_3$  in our test,

which might enhance the corrosion resistance of the steel and increase the critical  $\text{Cl}^-$  concentration in the solutions with the same pH value according to the above report.

### 3.4. Surface morphology of reinforcing steel

In order to further verify the above results obtained by electrochemical measurements, the surface morphology of the reinforcing steel immersed in the SCP solutions with different  $\text{Cl}^-$  concentrations was examined by SEM and shown in Figure 5. It can be seen from Figure 5(a) that the steel surface was smooth and no corrosion pits on it after it was immersed in the SCP solution without  $\text{Cl}^-$ , suggesting the steel was in a passive state. For the SCP solution with 0.40 M  $\text{Cl}^-$ , the steel surface got a little rough as shown in Figure 5(b), suggesting the stability of the passive film decreased. However, some obvious corrosion pits appeared on the surface of the steel after immersion in the SCP solution with 0.50 M  $\text{Cl}^-$ , indicating that localized corrosion (pitting) had occurred on the steel surface as shown in Figure 5(c). These results showed that the SEM analysis of the reinforcing steel surface was consistent with electrochemical measurements for the effect of the  $\text{Cl}^-$  concentration on the steel corrosion behavior, suggesting the critical  $\text{Cl}^-$  concentration of the steel immersed in the above alkali solution (pH 12.50) was 0.40-0.50 M.

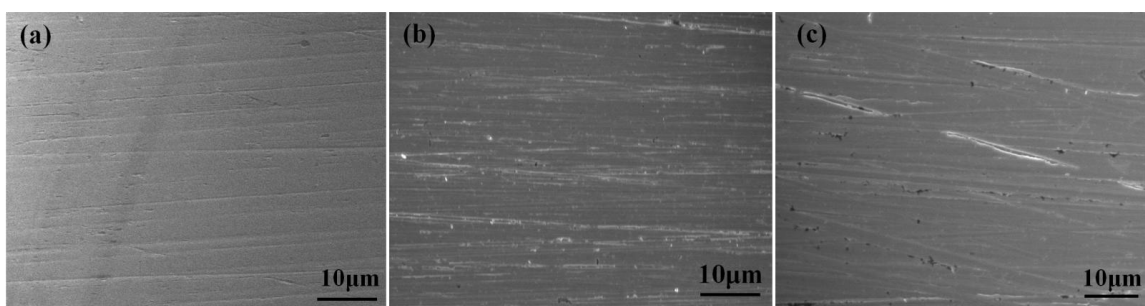


**Figure 5.** SEM images of the reinforcing steel surface after immersion in the SCP solutions with different  $\text{Cl}^-$  concentrations for 40 min, (a) without  $\text{Cl}^-$ , (b) 0.40 M  $\text{Cl}^-$ , (c) 0.50 M  $\text{Cl}^-$

### 3.5. XPS surface analysis

XPS analysis was used to study the effect of  $\text{Cl}^-$  on the corrosion behavior of reinforcing steel in SCP solutions by detecting the composition of reinforcing steel surface films. Figure 6 exhibits the XPS spectra for the major metal element ( $\text{Fe } 2p_{3/2}$ ) of surface films on reinforcing steel specimens after immersion 40 min in SCP solutions with different  $\text{Cl}^-$  concentrations. Figure 6(d) shows the relative atom fraction of Fe with different oxidation states identified by deconvolution for Figure 6(a-c). The peak at 706.9 eV was assigned to metallic Fe [26], and the peak at 708.2 eV was characteristic for  $\text{Fe}_3\text{O}_4$  [27], which was a mixture of  $\text{Fe}^{2+}$  and  $\text{Fe}^{3+}$ . The peak of higher binding energy at 710.7 eV was characteristic for ferric compounds [28]. It has been reported that the composition of the passive film of reinforcing steel is mainly ferric compounds [1,29-31]. When the film was destroyed, the corrosion

product on the film is mainly composed of ferrous compounds [1,32]. Therefore, we can determine the change trend of the corrosion behavior of reinforcing steel by detecting the change in  $\text{Fe}^{2+}$  and  $\text{Fe}^{3+}$  contents in the steel surface film. It can be seen from Figure 6(d) that the composition of the passive film on the steel immersed in the SCP solution without  $\text{Cl}^-$  contained the higher molar percentage of  $\text{Fe}^{3+}$ , whereas the molar percentages of Fe and  $\text{Fe}^{2+}$  were much lower. For the immersion in the solution with 0.40 M  $\text{Cl}^-$ , the molar percentage of  $\text{Fe}^{3+}$  somewhat decreased but remained above 30%, and the molar percentages of Fe and  $\text{Fe}^{2+}$  increased, which indicated the stability of the passive film on the steel was reduced. After the steel immersed in the SCP solutions with 0.50 M  $\text{Cl}^-$ , the molar percentage of  $\text{Fe}^{3+}$  reduced significantly, only 23.57%, while the molar percentage of Fe and  $\text{Fe}^{2+}$  were increased, especially metallic Fe content increased to 41.62%. It suggested that the passive film on the reinforcing steel surface was destroyed, the localized corrosion took place and resulted in some steel substrate was exposed to the test solution. Therefore, the result of the XPS analysis is consistent with the electrochemical measurements.

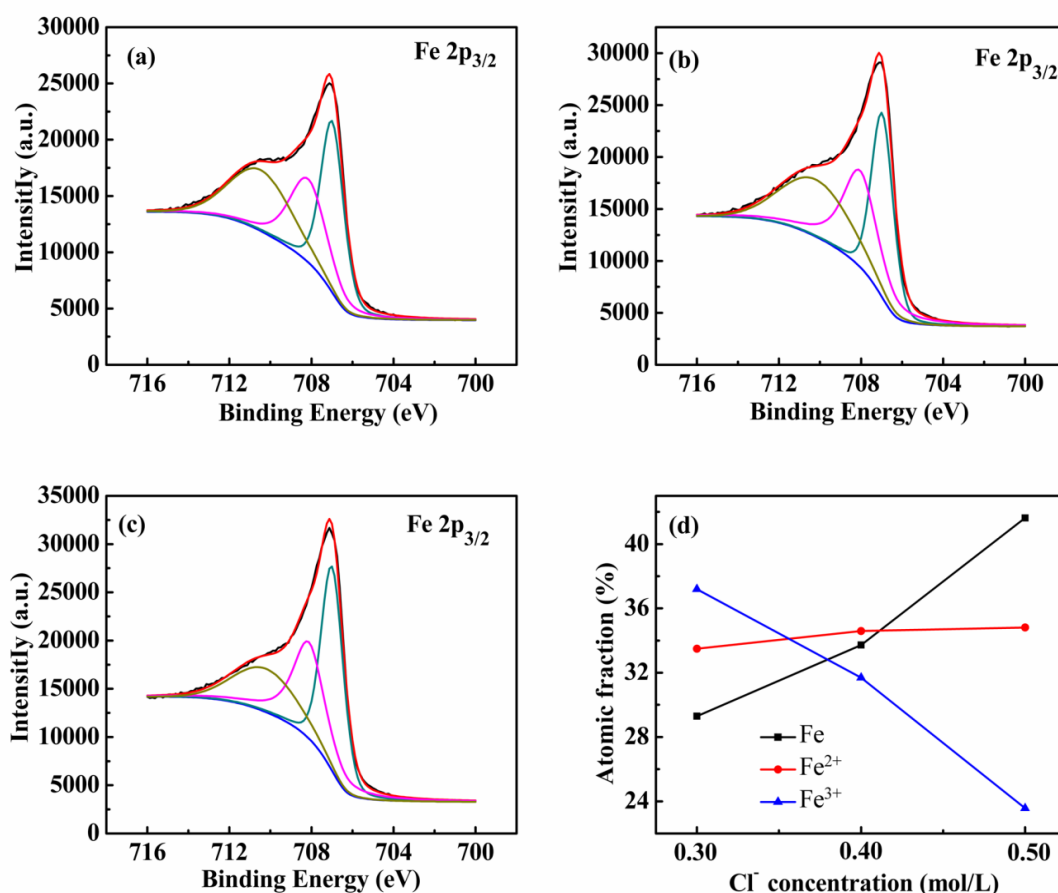


**Figure 6.** XPS deconvoluted profiles of Fe 2p<sub>3/2</sub> for the reinforcing steel surface film after 40 min immersion in the SCP solutions (a) without  $\text{Cl}^-$ , (b) with 0.40 M  $\text{Cl}^-$ , (c) with 0.50 M  $\text{Cl}^-$ , and (d) the relative atomic fraction of different valence states of Fe.

#### 4. CONCLUSIONS

The corrosion resistance of reinforcing steel was correlated with the  $\text{Cl}^-$  concentration in the simulated concrete pore solution with 0.6 M KOH, 0.2 M NaOH and 0.001 M  $\text{Ca}(\text{OH})_2$ . With the increase of the  $\text{Cl}^-$  concentration, the corrosion potential of the reinforcing steel shifted negatively, its corrosion current density increased, and polarization resistance decreased, suggesting the corrosion resistance of the steel was reduced.

The  $\text{Fe}^{3+}$  content in the steel surface film was higher when the steel in a passive state. The molar percentage of  $\text{Fe}^{3+}$  was reduced significantly, and the molar percentages of Fe and  $\text{Fe}^{2+}$  increased after immersion in the solution with 0.50 M  $\text{Cl}^-$ .

Electrochemical measurements, SEM and XPS analyses showed that the critical  $\text{Cl}^-$  concentration for the localized corrosion of the reinforcing steel was 0.40-0.50 M.

#### ACKNOWLEDGMENTS

This work was supported by the National Natural Science Foundation of China (Nos. 21073151, 21021002, 21173177, J1310024, 21203158), and the National High Technology Research and Development Program of China (2009AA03Z327).

#### References

1. V. Kumar, *Corros. Rev.*, 16, (1998) 317.
2. K. Thangavel, *Corros. Rev.*, 22, (2004) 55.
3. B. Huet, V. L'Hostis, F. Miserque and H. Idrissi, *Electrochim. Acta.*, 51, (2005) 172.
4. H. Xu, Y. Liu, W. Chen, R. G. Du and C. J. Lin, *Electrochim. Acta.*, 54, (2009) 4067.
5. A. Ueli, E. Bernhard, L. Claus K. and V. Oystein, *Electrochim. Acta.*, 56, (2011) 5877.
6. K. Y. Ann and H. W. Song, *Corros. Sci.*, 49, (2007) 4113.
7. D. A. Koleva, K. van Breugel, J. H. W. de Wit, E van Westing, N Boshkov and A. L. A Fraaij, *J. Electrochem. Soc.*, 154, (2007) E45.
8. L. Bertolini, F. Bolzoni, M. Gastaldi, T. Pastore, P. Pedferri and E. Redaelli, *Electrochim. Acta.*, 54, (2009) 1452.
9. M. Moreno, W. Morris, M. G. Alvarez and G. S. Duffo, *Corros. Sci.*, 46, (2004) 2681.
10. D. Izquierdo, C. Alonso, C. Andrade and M. Castellote, *Electrochim. Acta.*, 49, (2004) 2731.
11. M. Saremi and E. Mahallati, *Cement Concrete Res.*, 32, (2002) 1915.
12. D. A. Lewis, *Some aspects of the corrosion of steel in concrete*. In Proc. 1st International Conf Met. Corr, London, (1962) 547.
13. V K Gouda, *Brit. Corros. J.*, 5, (1970) 198.
14. W. Morris, A. Vico and A. Vazquez, *Electrochim. Acta.*, 49, (2004) 4447.
15. C. J. Kitowski and H. G. Wheat, *Corrosion*, 53, (1997) 216.

16. A. Poursaee and C. M. Hansson, *Cement Concrete Res.*, 37, (2007) 1127.
17. W. John. McCarter and O. Vennesland, *Constr. Build. Mater.*, 18, (2004) 351.
18. W. Morris, A. Vico, M. Vazquez and S. R. de Sanchez, *Corros Sci.*, 44, (2002) 81.
19. H. kaesche, *Corrosion of metals: Physicochemical Principles and Current Problems*, Springer, Heidelberg, Berlin(2003).
20. W. Chen, R. G. Du, C. Q. Ye, Y. F. Zhu, C. J. Lin, *Electrochim. Acta*, 55, (2010)5677.
21. S. A. Austin, R. Lyons, M. J. Ing, *Corrosion* 60 (2004) 203.
22. L. Hamadou, A. Kadri and N. Benbrahim, *Appl. Surf. Sci.*, 252, (2005) 1510.
23. L. Li, and A. A. Sagues., *ORROSION/99. NACE*, 567 (1999).
24. L. Bertolini, M. Gastaldi, M. P. Pedferri, P. Pedferri and T. Pastore, *Proc. Int. Conf. on Corrosion and Rehabilitation of Reinforced Concrete Structures*, Orlando, FL, USA, (1998).
25. J. G. N. Thomas, J. D. Davies, *Brit. Corros. J.*, 12, (1977)108.
26. P. Ghods, O. Burkan Isgor, F. Bensebaa and D. Kingston, *Corros Sci.*, 58, (2012)159.
27. Y. B. Hu, C. F. Dong, M. Sun, K. Xiao, P. Zhong and X. G. Li, *Corros Sci.*, 53, (2011)4159.
28. H. Luo, C. F. Dong, X. G. Li and K. Xiao, *Electrochim. Acta.*, 64, (2012)211.
29. Y. J. Kim, *Corrosion*, 55, (1999)81.
30. V. Schroeder and T. M. Devine, *J. Electrochem. Soc.*, 146, (1999)4061.
31. Z. F. Yin, W. Z. Zhao, Z. Q. Bai, Y. R. Feng and W. J. Zhou, *Electrochim. Acta.*, 53, (2008)3690.
32. G. M. Atenas, E. Mielczarski and J. A. Mielczarski, *J. Colloid Interface Sci.*, 289, (2005)157.